

Hard Non-Monotonic Attention for Character-Level Transduction

Shijie Wu[ⓐ] Pamela Shapiro[ⓐ] Ryan Cotterell^{ⓐ,ⓑ}

[ⓐ]Department of Computer Science, Johns Hopkins University, Baltimore, USA

[ⓑ]The Computer Laboratory, University of Cambridge, Cambridge, UK
{shijie.wu, pshapiro, ryan.cotterell}@jhu.edu

Abstract

Character-level string-to-string transduction is an important component of various NLP tasks. The goal is to map an input string to an output string, where the strings may be of different lengths and have characters taken from different alphabets. Recent approaches have used sequence-to-sequence models with an attention mechanism to learn which parts of the input string the model should focus on during the generation of the output string. Both soft attention and hard monotonic attention have been used, but hard non-monotonic attention has only been used in other sequence modeling tasks such as image captioning (Xu et al., 2015), and has required a stochastic approximation to compute the gradient. In this work, we introduce an exact, polynomial-time algorithm for marginalizing over the exponential number of non-monotonic alignments between two strings, showing that hard attention models can be viewed as neural reparameterizations of the classical IBM Model 1. We compare soft and hard non-monotonic attention experimentally and find that the exact algorithm significantly improves performance over the stochastic approximation and outperforms soft attention. Code is available at <https://github.com/shijie-wu/neural-transducer>.

1 Introduction

Many natural language tasks are expressible as string-to-string transductions operating at the character level. Probability models with recurrent neural parameterizations currently hold the state of the art on many such tasks. On those string-to-string transduction tasks that involve a mapping between two strings of different lengths, it is often necessary to resolve which input symbols are related to which output symbols. As an example, consider the task of transliterating a Russian word into the Latin alphabet. In many cases, there exists a one-to-two mapping between Cyrillic and Latin letters: in *Хрущёв* (*Khrushchev*), the Russian *X* can be considered to generate the Latin letters *Kh*. Supervision is rarely, if ever, provided at the level of character-to-character alignments—this is the problem that attention seeks to solve in neural models.

With the rise of recurrent neural networks, this problem has been handled with “soft” **attention** rather than traditional hard **alignment**. Attention (Bahdanau et al., 2015) is often described as “soft,” as it does not clearly associate a single input symbol with each output symbol, but rather offers a fuzzy notion of what input symbols may be responsible for which symbols in the output. In contrast, an alignment directly associates a given input symbol with a given output symbol. To express uncertainty, practitioners often place a distribution over the exponential number of hard non-monotonic alignments, just as a probabilistic parser places a distribution over an exponential number of trees. The goal, then, is to learn the parameters of this distribution over all non-monotonic alignments through backpropagation. Incorporating hard alignment into probabilistic transduction models dates back much farther in the NLP literature; arguably, originating with the seminal paper by Brown et al. (1993). Some neural approaches have moved back towards this approach of a more rigid alignment, referring to it as “hard attention.” We will refer to this as “hard attention” and to more classical approaches as “alignment.”

This paper offers two insights into the usage of hard alignment. First, we derive a dynamic program for the exact computation of the likelihood in a neural model with latent hard alignment: Previous work has used a stochastic algorithm to approximately sum over the exponential number of alignments between strings. In so doing, we go on to relate neural hard alignment models to the classical IBM Model 1 for alignment in machine translation. Second, we provide an experimental comparison that indicates hard attention models outperform soft attention models on three character-level string-to-string transduction tasks: grapheme-to-phoneme conversion, named-entity transliteration and morphological inflection.

2 Non-Monotonic Transduction

This paper presents a novel, neural, probabilistic latent-variable model for **non-monotonic** transduction. As a concrete example of a non-monotonic

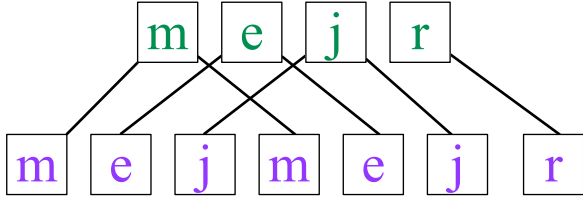


Figure 1: Example of a non-monotonic character-level transduction from the Micronesian language of Pingelapese. The infinitive *mejr* is mapped through a reduplicative process to its gerund *mejmejr* (Rehg and Sohl, 1981). Each input character is drawn in green and each output character is drawn in purple, connected with a line to the corresponding input character.

transduction, consider the mapping of a Pingelapese infinitive to its gerund, as shown in Fig. 1. The mapping requires us to generate the output string left-to-right, bouncing around the input string out-of-order to determine the characters to transduce from. As the non-monotonic alignment is the latent variable, we will face a combinatorial problem: summing over all non-monotonic alignments. The algorithmic contribution of this paper is the derivation of a simple dynamic program for computing this sum in polynomial time that still allows for very rich recurrent neural featurization of the model. With respect to the literature, our paper represents the first instance of exact marginalization for a neural transducer with hard non-monotonic alignment; previous methods, such as Rastogi et al. (2016) and Aharoni and Goldberg (2017), are exclusively monotonic.

Non-monotonic methods dominate character-level transduction. Indeed, the state of art in classic character-level NLP tasks such as grapheme-to-phoneme conversion (Yao and Zweig, 2015), transliteration (Rosca and Breuel, 2016) and morphological inflection generation (Kann and Schütze, 2016) is held by the soft non-monotonic method of Bahdanau et al. (2015). Even though non-monotonicity is more common in word-level tasks, it also exists in character-level transduction tasks, as evidenced by our example in Fig. 1 and the superior performance of non-monotonic methods. Our error analysis in §8.4 sheds some light on why non-monotonic methods are the state of the art in a seemingly monotonic task.

A Note on the Character-level Focus. A natural question at this point is why we are not experimenting with word-level transduction tasks, such as machine translation. As we show in the §3.2 our method is often an order of magnitude slower than standard soft attention. Thus, the exact marginalization scheme is practically unworkable for machine

translation; we discuss future extensions for machine translation in §6. However, the slow-down is no problem for character-level tasks and we show empirical gains in §8.

3 Hard Non-Monotonic Alignment

3.1 The Latent-Variable Model

An alphabet is a finite, non-empty set. Given two alphabets $\Sigma_x = \{x_1, \dots, x_{|\Sigma_x|}\}$ and $\Sigma_y = \{y_1, \dots, y_{|\Sigma_y|}\}$, probabilistic approaches to the problem attempt to estimate a probability distribution $p(\mathbf{y} | \mathbf{x})$ where $\mathbf{y} \in \Sigma_y^*$ and $\mathbf{x} \in \Sigma_x^*$. Foreshadowing, we will define the parameters of p to be, in part, the parameters of a recurrent neural network, in line with the state-of-the-art models. We define the set $\mathcal{A} = \{1, \dots, |\mathbf{x}|\}^{|\mathbf{y}|}$, which has an interpretation as the set of all (potentially non-monotonic) alignments from \mathbf{x} to \mathbf{y} with the implicit constraint that each output symbol y_i aligns to exactly one symbol in $\mathbf{x} \in \Sigma_x^*$. In other words, \mathcal{A} is the set of all many-to-one alignments between \mathbf{x} and \mathbf{y} where many may be as few as zero. We remark that $|\mathcal{A}| = |\mathbf{x}|^{|\mathbf{y}|}$, which is exponentially large in the length of the target string \mathbf{y} . For an $\mathbf{a} \in \mathcal{A}$, $A_i = a_i$ refers to the event that y_i , the i^{th} component of \mathbf{y} , is aligned to x_{a_i} , the a_i^{th} component of \mathbf{x} .

We define a probability distribution over output strings \mathbf{y} conditioned on an input string \mathbf{x} where we marginalize out *unobserved* alignments \mathbf{a} :

$$p(\mathbf{y} | \mathbf{x}) = \sum_{\mathbf{a} \in \mathcal{A}} p(\mathbf{y}, \mathbf{a} | \mathbf{x}) \quad (1a)$$

$$= \sum_{\mathbf{a} \in \mathcal{A}} \prod_{i=1}^{|\mathbf{y}|} p(y_i | a_i, \mathbf{y}_{<i}, \mathbf{x}) p(a_i | \mathbf{y}_{<i}, \mathbf{x}) \quad (1b)$$

exponential number of terms

$$= \prod_{i=1}^{|\mathbf{y}|} \sum_{a_i=1}^{|\mathbf{x}|} p(y_i | a_i, \mathbf{y}_{<i}, \mathbf{x}) p(a_i | \mathbf{y}_{<i}, \mathbf{x}) \quad (1c)$$

polynomial number of terms

$$= \prod_{i=1}^{|\mathbf{y}|} \sum_{j=1}^{|\mathbf{x}|} \alpha_j(i) p(y_i | j, \mathbf{y}_{<i}, \mathbf{x}) \quad (1d)$$

where the transition from (1a) to (1b) follows from the independence assumption and we define $\alpha_j(i) = p(a_i | \mathbf{y}_{<i}, \mathbf{x})$ and substitute $j = a_i$, in order to better notationally compare our model to that of Bahdanau et al. (2015) in §5. Each distribution $p(y_i | j, \mathbf{y}_{<i}, \mathbf{x})$ in the definition of the model has a clean interpretation as a distribution

over the output vocabulary Σ_y , given an input string $\mathbf{x} \in \Sigma_x^*$, where y_i is aligned to x_j . Thus, one way of thinking about this hard alignment model is as a product of mixture models, one mixture at each step, with mixing coefficients $\alpha_j(i)$.

A Note on EOS. We suppressed EOS in the autoregressive models above for brevity, e.g., $p(y_i | j, \mathbf{y}_{<i}, \mathbf{x})$ is a distribution over $\Sigma_y \cup \{\text{EOS}\}$, in order for $p(\mathbf{y} | \mathbf{x})$ to be a probability distribution.

Why Does Dynamic Programming Work? Our dynamic program to compute the likelihood, fully specified in eq. (1c), is quite simple: The non-monotonic alignments are independent of each other, i.e., $\alpha_j(i)$ is independent of $\alpha_j(i-1)$, conditioned on the observed sequence \mathbf{y} . This means that we can cleverly rearrange the terms in eq. (1b) using the distributive property. Were this not the case, we could not do better than having an exponential number of summands. This is immediately clear when we view our model as a graphical model, as in Fig. 2: There is no active trail from a_i to a_k where $k > i$, ignoring the dashed lines. Note that this is no different than the tricks used to achieve exact inference in n^{th} -order Markov models—one makes an independence assumption between the current bit of structure and the previous bits of structure to allow an efficient algorithm. For a proof of eq. (1b)–eq. (1c), one may look in Brown et al. (1993). Foreshadowing, we note that certain parameterizations make use of input feeding (Luong et al., 2015, §3.3), which breaks this independence; see §5.1.

Relation to IBM Model 1. The derivation above is similar to that of the IBM alignment model 1. We remark, however, two key generalizations that will serve our recurrent neural parameterization well in §4. First, traditionally, derivations of IBM Model 1 omits a prior over alignments $p(a_i | \mathbf{x})$, taking it to be uniform. Due to this omission, an additional multiplicative constant $\varepsilon/|\mathbf{x}|^{|\mathbf{y}|}$ is introduced to ensure the distribution remains normalized (Koehn, 2009). Second, IBM Model 1 does not condition on previously generated words on the output side. In other words, in their original model, Brown et al. (1993) assume that $p(y_i | a_i, \mathbf{y}_{<i}, \mathbf{x}) = p(y_i | a_i, \mathbf{x})$, forsaking dependence on $\mathbf{y}_{<i}$. We note that there is no reason why we need to make this independence assumption—we will likely want a target-side language model in transduction. Indeed, subsequent statistical machine translation systems, e.g., MOSES (Koehn

et al., 2007), integrate a language model into the decoder. It is of note that many models in NLP have made similar independence assumptions, e.g., the emission distribution hidden Markov models (HMMs) are typically taken to be independent of all previous emissions (Rabiner, 1989). These assumptions are generally not necessary.

3.2 Algorithmic Analysis: Time Complexity

Let us assume that the requisite probability distributions are computable in $\mathcal{O}(1)$ time and the softmax takes $\mathcal{O}(|\Sigma_y|)$. Then, by inspection, the computation of the distribution in eq. (1d) is $\mathcal{O}(|\mathbf{x}| \cdot |\mathbf{y}| \cdot |\Sigma_y|)$, as the sum in eq. (1c) contains this many terms thanks to the dynamic program that allowed us to rearrange the sum and the product. While this “trick” is well known in the NLP literature—it dates from the seminal work in statistical machine translation by Brown et al. (1993)—it has been forgotten in recent formulations of hard alignment (Xu et al., 2015), which use stochastic approximation to handle the exponential summands. As we will see in §5, we can compute the soft-attention model of Bahdanau et al. (2015) in $\mathcal{O}(|\mathbf{x}| \cdot |\mathbf{y}| + |\mathbf{y}| \cdot |\Sigma_y|)$ time. When Σ_y is large, for example in the case of machine translation with tens of thousands of Σ_y at least, we can ignore $|\mathbf{x}| \cdot |\mathbf{y}|$ in soft-attention model, and the exact marginalization has an extra $|\mathbf{x}|$ -factor compared to soft-attention model. In practice, Shi and Knight (2017) show the bottleneck of an NMT system is the softmax layer, making the extra $|\mathbf{x}|$ -factor practically cumbersome.

4 Recurrent Neural Parameterization

How do we parameterize $p(y_i | a_i, \mathbf{y}_{<i}, \mathbf{x})$ and $\alpha_j(i)$ in our hard, non-monotonic transduction model? We will use a neural network identical to the one proposed in the attention-based sequence-to-sequence model of Luong et al. (2015) *without input feeding* (a variant of Bahdanau et al. (2015)).

4.1 Encoding the Input

All models discussed in this exposition will make use of the same mechanism for mapping a source string $\mathbf{x} \in \Sigma_x^*$ into a fixed-length representation in \mathbb{R}^{d_h} . This mapping will take the form of a bidirectional recurrent neural network encoder, which works as follows: each element of Σ_x is mapped to an embedding vector of length d_e through a mapping: $\mathbf{e} : \Sigma_x \rightarrow \mathbb{R}^{d_e}$. Now, the RNN folds the

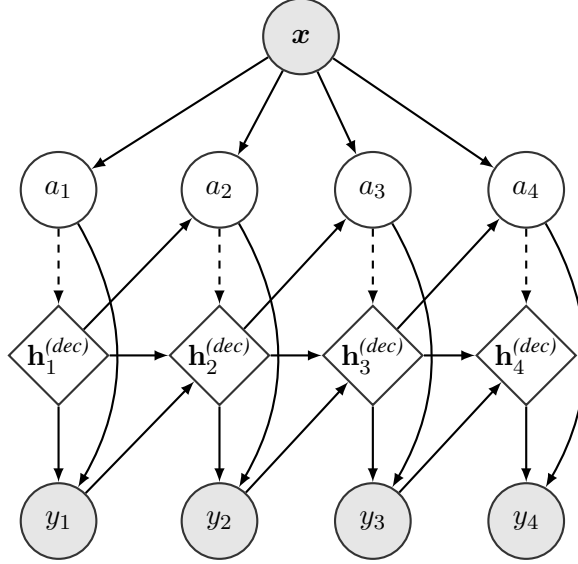


Figure 2: Our hard-attention model *without input feeding* viewed as a graphical model. Note that the circular nodes are random variables and the diamond nodes are deterministic variables ($\mathbf{h}_i^{(dec)}$ is first discussed in §4.3). The independence assumption between the alignments a_i when the y_i are *observed* becomes clear. Note that we have omitted arcs from x to $y_1, y_2, y_3,$ and y_4 for clarity (to avoid crossing arcs). We alert the reader that the dashed edges show the additional dependencies added in the *input feeding version*, as discussed in §5.1. Once we add these in, the a_i are no longer independent and break exact marginalization. Note the hard-attention model does not enforce an exact one-to-one constraint. Each source-side word is free to align with many of the target-side words, independent of context. In the latent variable model, the x variable is a vector of source words, and the alignment may be over more than one element of x .

following recursion over the string x left-to-right:

$$\vec{\mathbf{h}}_j^{(enc)} = \tanh \left(\vec{\mathbf{U}}^{(enc)} \mathbf{e}^{(enc)}(x_j) + \vec{\mathbf{V}}^{(enc)} \vec{\mathbf{h}}_{j-1}^{(enc)} + \vec{\mathbf{b}}^{(enc)} \right) \quad (2)$$

where we fix the 0th hidden state $\mathbf{h}_0^{(enc)}$ to the zero vector and the matrices $\vec{\mathbf{U}}^{(enc)} \in \mathbb{R}^{d_h \times d_e}$, $\vec{\mathbf{V}}^{(enc)} \in \mathbb{R}^{d_h \times d_h}$ and the bias term $\vec{\mathbf{b}}^{(enc)} \in \mathbb{R}^{d_h}$ are parameters to be learned. Performing the same procedure on the reversed string and using an RNN with different parameters, we arrive at hidden state vectors $\overleftarrow{\mathbf{h}}_j^{(enc)}$. The final hidden states from the encoder are the concatenation of the two, i.e., $\mathbf{h}_j^{(enc)} = \vec{\mathbf{h}}_j^{(enc)} \oplus \overleftarrow{\mathbf{h}}_j^{(enc)}$, where \oplus is vector concatenation.

As has become standard, we will use an extension to this recursion: we apply the long short-term memory (LSTM; Hochreiter and Schmidhuber, 1997) recursions, rather than those of a vanilla RNN (Elman network; Elman, 1990).

4.2 Parameterization.

Now, we define the alignment distribution

$$\alpha_j(i) = \frac{\exp(e_{ij})}{\sum_{j'=1}^{|\mathbf{x}|} \exp(e_{ij'})} \quad (3a)$$

$$e_{ij} = \mathbf{h}_i^{(dec)\top} \mathbf{T} \mathbf{h}_j^{(enc)} \quad (3b)$$

where $\mathbf{T} \in \mathbb{R}^{d_h \times 2d_h}$ and $\mathbf{h}_i^{(dec)}$, the decoder RNN's hidden state, is defined in §4.3. Importantly, the alignment distribution $\alpha_j(i)$ at time step i will *only* depend on the prefix of the output string $\mathbf{y}_{<i}$ generated so far. This is clear since the output-side decoder is a unidirectional RNN. We also define

$$p(y_i | a_i, \mathbf{y}_{<i}, \mathbf{x}) = \text{softmax}_{y_i} \left(\mathbf{W} \mathbf{f}(\mathbf{h}_i^{(dec)}, \mathbf{h}_{a_i}^{(enc)}) \right) \quad (4)$$

The function \mathbf{f} is a non-linear and vector-valued; one popular choice of \mathbf{f} is a multilayer perceptron with parameters to be learned. We define

$$\mathbf{f}(\mathbf{h}_i^{(dec)}, \mathbf{h}_{a_i}^{(enc)}) = \tanh \left(\mathbf{S} (\mathbf{h}_i^{(dec)} \oplus \mathbf{h}_{a_i}^{(enc)}) \right) \quad (5)$$

where $\mathbf{S} \in \mathbb{R}^{d_s \times 3d_h}$.

4.3 Updating the hidden state $\mathbf{h}_i^{(dec)}$

The hidden state $\mathbf{h}_i^{(dec)}$ is also updated through the LSTM recurrences (Hochreiter and Schmidhuber, 1997). The RNN version of the recurrence mirrors that of the encoder,

$$\mathbf{h}_i^{(dec)} = \tanh \left(\mathbf{U}^{(dec)} \mathbf{e}^{(dec)}(y_{i-1}) + \mathbf{V}^{(dec)} \mathbf{h}_{i-1}^{(dec)} + \mathbf{b}^{(dec)} \right) \quad (6)$$

where $\mathbf{e}^{(dec)} : \Sigma_y \rightarrow \mathbb{R}^{d_e}$ produces an embedding of each of the symbols in the output alphabet. What is crucial about this RNN, like the $\alpha_j(i)$, is that it only summarizes the characters decoded so far *independently of the previous attention weights*. In other words, the attention weights at time step i will have no influence from the attention weights at previous time steps, shown in Fig. 2. This is what allows for dynamic programming.

5 Transduction with Soft Attention

In order to contrast it with the hard alignment mechanism we develop, we here introduce Luong attention (Luong et al., 2015) for recurrent neural sequence to sequence models (Sutskever et al., 2014). Note that this model will also serve as an experimental baseline in §8.

The soft-attention transduction model defines a distribution over the output Σ_y^* , much like the hard-attention model, with the following expression:

$$p(\mathbf{y} | \mathbf{x}) = p(\text{EOS} | \mathbf{y}, \mathbf{x}) \prod_{i=1}^{|\mathbf{y}|} p(y_i | \mathbf{y}_{<i}, \mathbf{x}) \quad (7)$$

where we define each conditional distribution as

$$p(y_i | \mathbf{y}_{<i}, \mathbf{x}) = \text{softmax}_{y_i} \left(\mathbf{W} \mathbf{f}(\mathbf{h}_i^{(dec)}, \mathbf{c}_i) \right) \quad (8)$$

over $\Sigma_y \cup \{\text{EOS}\}$. We reuse the function \mathbf{f} in eq. (5). The hidden state $\mathbf{h}_i^{(dec)}$, as before, is the i^{th} state of a target-side language model that summarizes the prefix of the string decoded so far; this is explained in §4.3. And, finally, we define the **context vector**

$$\mathbf{c}_i = \sum_{j=1}^{|\mathbf{x}|} \alpha_j(i) \mathbf{h}_j^{(enc)} \quad (9)$$

using the same alignment distribution as in §4.2. In the context of the soft-attention model, this distribution is referred to as the **attention weights**.

Inspection shows that there is only a small difference between the soft-attention model presented here and our hard non-monotonic attention model. The difference is where we place the probabilities $\alpha_j(i)$. In the soft-attention version, we place them inside the softmax (and the function \mathbf{f}), as in eq. (8), and we have a mixture of the encoder’s hidden states, the context vector, that we feed into the model. On the other hand, if we place them outside the softmax, we have a mixture of softmaxes, as shown in eq. (1c). Both models have *identical* set of parameters.

5.1 Input Feeding: What’s That?

The equations in eq. (6), however, are not the only approach. **Input-feeding** is another popular approach that is, perhaps, standard at this point (Luong et al., 2015). Input feeding refers to the setting where the architecture designer additionally feeds the attention weights into the update for the decoder’s hidden state. This yields the recursion

$$\mathbf{h}_i^{(dec)} = \tanh \left(\mathbf{U}^{(dec)} (\mathbf{e}^{(dec)}(y_{i-1}) \oplus \bar{\mathbf{c}}_{i-1}) + \mathbf{V}^{(dec)} \mathbf{h}_{i-1}^{(dec)} + \mathbf{b}^{(dec)} \right) \quad (10)$$

where $\bar{\mathbf{c}}_{i-1} = \mathbf{f}(\mathbf{h}_{i-1}^{(dec)}, \mathbf{c}_{i-1})$. Note that this requires that $\mathbf{U}^{(dec)} \in \mathbb{R}^{d_h \times (d_e + d_s)}$. This is the architecture discussed in Bahdanau et al. (2015, §3.1). In contrast to the architecture above, this architecture has attention weights that do depend on previous attention weights due to the feeding in of the context vector \mathbf{c}_i . See Cohn et al. (2016) for another attempt to incorporate structural biases directly into the attention mechanism such that the attention distribution is influenced by previous attention distributions.

5.2 Combining Hard Non-Monotonic Attention with Input Feeding

To combine hard attention with input feeding, Xu et al. (2015) derive a variational lower bound on the log-likelihood through Jensen’s inequality:

$$\log p(\mathbf{y} | \mathbf{x}) = \log \sum_{\mathbf{a} \in \mathcal{A}} p(\mathbf{y}, \mathbf{a} | \mathbf{x}) \quad (11a)$$

$$= \log \sum_{\mathbf{a} \in \mathcal{A}} p(\mathbf{a} | \mathbf{x}) p(\mathbf{y} | \mathbf{x}, \mathbf{a}) \quad (11b)$$

$$\geq \sum_{\mathbf{a} \in \mathcal{A}} p(\mathbf{a} | \mathbf{x}) \log p(\mathbf{y} | \mathbf{x}, \mathbf{a}) \quad (11c)$$

Note that we have omitted the dependence of $p(\mathbf{a} | \mathbf{x})$ on the appropriate prefix of \mathbf{y} ; this was done for notational simplicity. Using this bound, Xu et al. (2015) derive an efficient approximation to the gradient using the REINFORCE trick of Williams (1992). This sampling-based gradient estimator is then used for learning but suffers from high variance. We compare our dynamic programming version to this model in §8.

6 Future Work

Just as Brown et al. (1993) started with IBM Model 1 and built up to richer models, we can

	source	target
Grapheme-to-phoneme conversion	a c t i o n	AE K SH AH N
Named-entity transliteration	A A C H E N	아 헨
Morphological inflection	N AT+ALL SG l i p u k e	l i p u k k e e l l e

Table 1: Example of source and target string for each task as processed by the model

do the same. Extensions, resembling those of IBM Model 2 and the HMM aligner (Vogel et al., 1996) that generalize IBM Model 1, are easily bolted onto our proposed model as well. If we are willing to perform approximate inference, we may also consider fertility as found in IBM Model 4.

In order to extend our method to machine translation (MT) in any practical manner, we require an approximation to the softmax. Given that the softmax is already the bottleneck of neural MT models (Shi and Knight, 2017), we can not afford ourselves a $\mathcal{O}(|x|)$ slowdown during training. Many methods have been proposed for approximating the softmax (Goodman, 2001; Bengio et al., 2003; Gutmann and Hyvärinen, 2010). More recently, Chen et al. (2016) compared methods on neural language modeling, and Grave et al. (2017) proposed a GPU-friendly method.

7 The Tasks

The empirical portion of the paper focuses on character-level string-to-string transduction problems. We consider three tasks: **G**: grapheme-to-phoneme conversion, **T**: named-entity transliteration, and **I**: morphological inflection. We describe each briefly in turn and we give an example of a source and target string for each task in Tab. 1.

Grapheme-to-Phoneme Conversion. We use the standard grapheme-to-phoneme conversion (G2P) dataset: the Sphinx-compatible version of CMUDict (Weide, 1998) and NetTalk (Sejnowski and Rosenberg, 1987). G2P transduces a word, a string of graphemes, to its pronunciation, a string of phonemes. We evaluate with word error rate (WER) and phoneme error rate (PER) (Yao and Zweig, 2015). PER is equal to the edit distance divided by the length of the string of phonemes.

Named-Entity Transliteration. We use the NEWS 2015 shared task on machine transliteration (Zhang et al., 2015) as our named-entity transliteration dataset. It contains 14 language pairs. Transliteration transduces a named entity from its source language to a target language—in other words,

	soft attention	hard alignment
input-fed	yes ① Bahdanau et al. (2015); Luong et al. (2015) ② Xu et al. (2015)	
input-not-fed	no ③ Luong et al. (2015) without input feeding	④ This work

Table 2: The 4 architectures considered in the paper.

from a string in the source orthography to a string in the target orthography. We evaluate with word accuracy in percentage (ACC) and mean F-score (MFS) (Zhang et al., 2015). For completeness, we include the definition of MFS in App. A.

Morphological Inflection. We consider the high-resource setting of task 1 in the CoNLL–SIGMORPHON 2017 shared task (Cotterell et al., 2017) as our morphological inflection dataset. It contains 51 languages in the high-resource setting. Morphological inflection transduces a lemma (a string of characters) and a morphological tag (a sequence of subtags) to an inflected form of the word (a string of characters). We evaluate with word accuracy (ACC) and average edit distance (MLD) (Cotterell et al., 2017).

8 Experiments

The goal of the empirical portion of our paper is to perform a controlled study of the different architectures and approximations discussed up to this point in the paper. §8.1 exhibits the neural architectures we compare and the main experimental results¹ are in Tab. 3. In §8.2, we present the experimental minutiae, e.g. hyperparameters. In §8.3, we analyze our experimental findings. Finally, in §8.4, we perform error analysis and visualize the soft attention weight and hard alignment distribution.

8.1 The Architectures

The four architectures we consider in controlled comparison are: ①: soft attention *with* input feeding, ②: hard attention *with* input feeding, ③: soft attention *without* input feeding and ④: **hard attention without input feeding** (our system). They are

¹Because we do not have access to the test set of **T**, we only report development performance.

	Grapheme-to-Phoneme Conversion (G)				Named-Entity Transliteration (T)				Morphological Inflection (I)			
	Small		Large		Small		Large		Small		Large	
	WER	PER	WER	PER	ACC	MFS	ACC	MFS	ACC	MLD	ACC	MLD
①	33.7	0.080	30.8	0.074	38.9	0.890	39.9	0.893	91.4	0.183	91.1	0.201
U	30.6	0.074	30.4	0.073	39.8	0.891	40.3	0.894	91.0	0.185	91.0	0.212
②	32.3	0.079	33.1	0.081	36.3	0.881	30.8	0.837	91.0	0.193	89.3	0.322
③	30.3	0.074	28.6	0.070	40.1	0.891	40.5	0.894	92.0	0.163	92.2	0.166
④	29.6	0.072	28.2	0.068	39.8	0.891	41.1	0.894	92.6	0.151	93.6	0.128
R	30.7	0.076	29.7	0.074	37.1	0.882	36.9	0.863	91.2	0.190	92.8	0.151
M	33.9	0.082	29.9	0.072	38.8	0.959	40.1	0.960	91.7	0.160	92.8	0.141

Table 3: Average test performance on G, T and I averaged across datasets and languages. See App. B for full breakdown.

	Small	Large	Search range
Emb. dim.	100	200	{50,100,200,300}
Enc. dim.	200	400	{100,200,400,600}
Enc. layer	1	2	{1,2,3}
Dec. dim.	200	400	{100,200,400,600}
Dec. layer	1	1	{1,2,3}
Dropout	0.2	0.4	{0,0.1,0.2,0.4}
# param.	1.199M	8.621M	N/A

Table 4: Model hyperparameters and search range

also shown in Tab. 2. As a fifth system, we compare to the monotonic system (M): Aharoni and Goldberg (2017). Additionally, we present (U), a variant of (1) where the number of parameters is not controlled for, and (R), a variant of (4) trained using REINFORCE instead of exact marginalization.

8.2 Experimental Details

We implement the experiments with PyTorch (Paszke et al., 2017) and we port the code of Aharoni and Goldberg (2017) to admit batched training. Because we did not observe any improvements in preliminary experiments when decoding with beam search², all models are decoded greedily.

Data Preparation. For G, we sample 5% and 10% of the data as development set and test set, respectively. For T, we only run experiments with 11 out of 14 language pairs³ because we do not have access to all the data.

Model Hyperparameters. The hyperparameters of all models are in Tab. 4. The hyperparameters of the large model are tuned using the baseline (3) on selected languages in I, and the search range is

²Compared to greedy decoding with an average error rate of 20.1% and an average edit distance of 0.385, beam search with beam size 5 gets a slightly better edit distance of 0.381 while hurting the error rate with 20.2%.

³Ar-En, En-Ba, En-Hi, En-Ja, En-Ka, En-Ko, En-Pe, En-Ta, En-Th, Jn-Jk and Th-En.

shown in Tab. 4. All three tasks have the same two sets of hyperparameters. To ensure that (1) has the same number of parameters as the other models, we decrease d_s in eq. (5) while for the rest of the models $d_s = 3d_h$. Additionally, we use a linear mapping to merge $e^{(dec)}(y_{i-1})$ and \bar{c}_{i-1} in eq. (10) instead of concatenation. The output of the linear mapping has the same dimension as $e^{(dec)}(y_{i-1})$, ensuring that the RNN has the same size.

(M) has quite a different architecture: The input of the decoder RNN is the concatenation of the previously predicted word embedding, the encoder’s hidden state at a specific step, and in the case of I, the encoding of the morphological tag. Differing from Aharoni and Goldberg (2017), we concatenate all attributes’ embeddings (0 for attributes that are not applicable) and merge them with a linear mapping. The dimension of the merged vector and attributes vector are d_e . To ensure that it has the same number of parameters as the rest of the model, we increase the hidden size of the decoder RNN.

Optimization. We train the model with Adam (Kingma and Ba, 2015) with an initial learning rate of 0.001. We halve the learning rate whenever the development log-likelihood doesn’t improve. We stop after the learning rate dips to 1×10^{-5} . We save all models after each epoch and select the model with the best development performance. We train the model for at most 50 epochs, though all the experiments stop early. We train on G, T, and I with batch sizes of 20, 50 and 20, respectively. We notice in the experiments that the training of (1) and (U) is quite unstable with the large model, probably because of the longer chain of gradient information flow. We apply gradient clipping to the large model with maximum gradient norm 5.

REINFORCE. In the REINFORCE training of (R) and (2), we sample 2 and 4 positions at each time

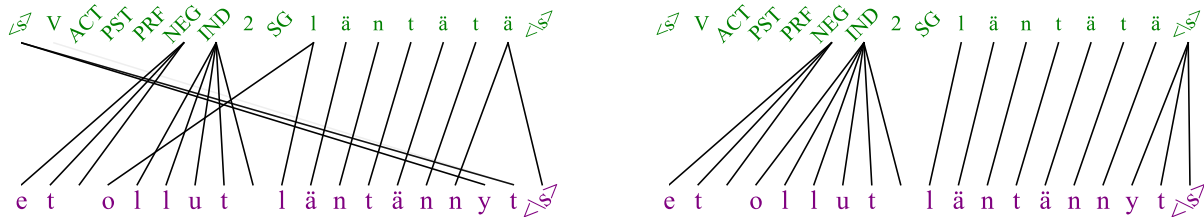


Figure 3: Attention-weight (3); left) and alignment distribution (4); right) of Finnish in I. Both models predict correctly.

step for the small and large models, respectively. The latter is tuned on selected languages in I with search range {2,3,4,5}. To stabilize the training, we apply a baseline with a moving average reward and discount factor of 0.9, similar to Xu et al. (2015).

8.3 Experimental Findings

Finding #1: Effect of Input Feeding. By comparing 3 and 4 against 1 and 2 in Tab. 3, we find input feeding hurts performance in all settings and all tasks. This runs in contrast to the reported results of Luong et al. (2015), but they experiment on machine translation, rather than character-level transduction. This validates our independence assumption about the alignment distribution.

Finding #2: Soft Attention vs. Hard Attention.

Training with REINFORCE hurts the performance of the hard attention model; compare 1 and 2 (trained with REINFORCE), in Tab. 3. On the other hand, training with exact marginalization causes the hard attention model to outperform the soft attention model in nearly all settings; compare 3 and 4 in Tab. 3. This comparison shows that hard attention outperforms soft attention in character-level string transduction when trained with exact marginalization.

Finding #3: Non-monotonicity vs. Monotonicity.

The monotonic model M underperforms compared to non-monotonic models 3 in Tab. 3 except for one setting. It performs slightly worse on T and G due to the many-to-one alignments in the data and the fact that Aharoni and Goldberg (2017) can only use the hidden vector of the final element of the span in a many-to-one alignment to directly predict the one target element. The current state-of-the-art systems for character-level string transduction are non-monotonic models, despite the tasks' seeming monotonicity; see §8.4.

Finding #4: Approximate Hard Attention.

Given our development of an exact marginalization

	NETtalk		CMUDict		✓	✗	✓	✗
	3	4	3	4				
Monotonic	18742	1230	18823	1172	95824	17294	96176	17159
Non-monotonic	31	5	12	1	158	162	37	66

Table 5: Breakdown of correct and incorrect predictions of monotonic and non-monotonic alignments of 3 and 4 in G, derived from the soft attention weights and the hard alignment distribution

method for neural models with hard attention, a natural question to ask is how much the exact marginalization helps during learning. By comparing 4 and R in Tab. 3, we observe that training with exact marginalization clearly outperforms training under stochastic approximation in every setting and on every dataset. We also observe that the exact marginalization allows faster convergence, since training with REINFORCE is quite unstable where some runs seemingly to get stuck.

Finding #5: Controlling for Parameters.

Input feeding yields a more expressive model, but also leads to an increase in the number of parameters. Here, we explore what effect this has on the performance of the models. In their ablation, Luong et al. (2015) did not control the number of parameters when adding input feeding. The total number of parameters of U is 1.679M for the small setting and 10.541M for the large setting, which has 40% and 22.3% more parameters than the controlled setting. By comparing 1 and U in Tab. 3, we find that the increase in parameters, rather than the increase in expressivity explains the success of input feeding.

8.4 Visualization and Error Analysis

We hypothesize that even though the model is non-monotonic, it can learn monotonic alignment with flexibility if necessary, giving state-of-the-art results on many seemingly monotonic character-level string transduction tasks. To show more insights, we compare the best soft attention model (3) against the best hard alignment model (4) on G by showing the confusion matrix of each model

in Tab. 5. An alignment is non-monotonic when alignment edges are predicted by the model cross. There is an edge connecting x_j and y_i if the attention weight or hard alignment distribution $\alpha_j(i)$ is larger than 0.1. We find that the better-performing transducers are more monotonic, and most learned alignments are monotonic. The results indicate that there are a few transductions that are indeed non-monotonic in the dataset. However, the number is so few that this does not entirely explain why non-monotonic models outperform the monotonic models. We speculate this lies in the architecture of Aharoni and Goldberg (2017), which does not permit many-to-one alignments, while monotonic alignment learned by the non-monotonic model is more flexible. Future work will investigate this.

In Fig. 3, we visualize the soft attention weights (3) and the hard alignment distribution (4) side by side. We observe that the hard alignment distribution is more interpretable, with a clear boundary when predicting the prefixes.

9 Conclusion

We exhibit an efficient dynamic program for the exact marginalization of all non-monotonic alignments in a neural sequence-to-sequence model. We show empirically that the exact marginalization helps over approximate inference by REINFORCE and that models with hard, non-monotonic alignment outperform those with soft attention.

Acknowledgements. RC was supported by an NDSEG fellowship and a Facebook Fellowship.

References

- Roei Aharoni and Yoav Goldberg. 2017. [Morphological inflection generation with hard monotonic attention](#). In *Proceedings of the 55th Annual Meeting of the Association for Computational Linguistics (Volume 1: Long Papers)*, pages 2004–2015, Vancouver, Canada. Association for Computational Linguistics.
- Dzmitry Bahdanau, Kyunghyun Cho, and Yoshua Bengio. 2015. [Neural machine translation by jointly learning to align and translate](#). In *International Conference on Learning Representations*, volume abs/1409.0473.
- Yoshua Bengio, Réjean Ducharme, Pascal Vincent, and Christian Jauvin. 2003. [A neural probabilistic language model](#). *Journal of Machine Learning Research*, 3:1137–1155.
- Peter F. Brown, Vincent J. Della Pietra, Stephen A. Della Pietra, and Robert L. Mercer. 1993. [The mathematics of statistical machine translation: Parameter estimation](#). *Computational Linguistics*, 19(2):263–311.
- Wenlin Chen, David Grangier, and Michael Auli. 2016. [Strategies for training large vocabulary neural language models](#). In *Proceedings of the 54th Annual Meeting of the Association for Computational Linguistics (Volume 1: Long Papers)*, pages 1975–1985, Berlin, Germany. Association for Computational Linguistics.
- Trevor Cohn, Cong Duy Vu Hoang, Ekaterina Vymolova, Kaisheng Yao, Chris Dyer, and Gholamreza Haffari. 2016. [Incorporating structural alignment biases into an attentional neural translation model](#). In *Proceedings of the 2016 Conference of the North American Chapter of the Association for Computational Linguistics: Human Language Technologies*, pages 876–885, San Diego, California. Association for Computational Linguistics.
- Ryan Cotterell, Christo Kirov, John Sylak-Glassman, Géraldine Walther, Ekaterina Vylomova, Patrick Xia, Manaal Faruqui, Sandra Kübler, David Yarowsky, Jason Eisner, and Mans Hulden. 2017. [CoNLL-SIGMORPHON 2017 shared task: Universal morphological reinflection in 52 languages](#). In *Proceedings of the CoNLL SIGMORPHON 2017 Shared Task: Universal Morphological Reinflection*, pages 1–30, Vancouver. Association for Computational Linguistics.
- Jeffrey L. Elman. 1990. [Finding structure in time](#). *Cognitive Science*, 14(2):179–211.
- Joshua Goodman. 2001. [Classes for fast maximum entropy training](#). In *IEEE International Conference on Acoustics, Speech, and Signal Processing Proceedings*, volume 1, pages 561–564. IEEE.
- Édouard Grave, Armand Joulin, Moustapha Cissé, David Grangier Facebook AI Research, and Hervé Jégou. 2017. [Efficient softmax approximation for GPUs](#). In *Proceedings of the 34th International Conference on Machine Learning*, pages 1302–1310.
- Michael Gutmann and Aapo Hyvärinen. 2010. [Noise-contrastive estimation: A new estimation principle for unnormalized statistical models](#). In *Proceedings of the Thirteenth International Conference on Artificial Intelligence and Statistics*, pages 297–304.
- Sepp Hochreiter and Jürgen Schmidhuber. 1997. [Long short-term memory](#). *Neural Computation*, 9(8):1735–1780.
- Katharina Kann and Hinrich Schütze. 2016. [Single-model encoder-decoder with explicit morphological representation for reinflection](#). In *Proceedings of the 54th Annual Meeting of the Association for Computational Linguistics (Volume 2: Short Papers)*, pages 555–560, Berlin, Germany. Association for Computational Linguistics.

- Diederick P. Kingma and Jimmy Ba. 2015. [Adam: A method for stochastic optimization](#). In *International Conference on Learning Representations*.
- Philipp Koehn. 2009. *Statistical Machine Translation*. Cambridge University Press.
- Philipp Koehn, Hieu Hoang, Alexandra Birch, Chris Callison-Burch, Marcello Federico, Nicola Bertoldi, Brooke Cowan, Wade Shen, Christine Moran, Richard Zens, Chris Dyer, Ondrej Bojar, Alexandra Constantin, and Evan Herbst. 2007. [Moses: Open source toolkit for statistical machine translation](#). In *Proceedings of the 45th Annual Meeting of the Association for Computational Linguistics Companion Volume Proceedings of the Demo and Poster Sessions*, pages 177–180, Prague, Czech Republic. Association for Computational Linguistics.
- Thang Luong, Hieu Pham, and Christopher D. Manning. 2015. [Effective approaches to attention-based neural machine translation](#). In *Proceedings of the 2015 Conference on Empirical Methods in Natural Language Processing*, pages 1412–1421, Lisbon, Portugal. Association for Computational Linguistics.
- Adam Paszke, Sam Gross, Soumith Chintala, Gregory Chanan, Edward Yang, Zachary DeVito, Zeming Lin, Alban Desmaison, Luca Antiga, and Adam Lerer. 2017. [Automatic differentiation in PyTorch](#). In *Autodiff Workshop (NeurIPs 2017 Workshop)*.
- Lawrence R. Rabiner. 1989. [A tutorial on hidden Markov models and selected applications in speech recognition](#). *Proceedings of the IEEE*, 77(2):257–286.
- Pushpendre Rastogi, Ryan Cotterell, and Jason Eisner. 2016. [Weighting finite-state transductions with neural context](#). In *Proceedings of the 2016 Conference of the North American Chapter of the Association for Computational Linguistics: Human Language Technologies*, pages 623–633, San Diego, California. Association for Computational Linguistics.
- Kenneth L. Rehg and Damian G. Sohl. 1981. *Ponapean Reference Grammar*. University of Hawaii Press.
- Mihaela Rosca and Thomas Breuel. 2016. [Sequence-to-sequence neural network models for transliteration](#). *arXiv preprint arXiv:1610.09565*.
- Terrence J. Sejnowski and Charles R. Rosenberg. 1987. [Parallel networks that learn to pronounce English text](#). *Complex Systems*, 1.
- Xing Shi and Kevin Knight. 2017. [Speeding up neural machine translation decoding by shrinking run-time vocabulary](#). In *Proceedings of the 55th Annual Meeting of the Association for Computational Linguistics (Volume 2: Short Papers)*, pages 574–579, Vancouver, Canada. Association for Computational Linguistics.
- Ilya Sutskever, Oriol Vinyals, and Quoc V. Le. 2014. [Sequence to sequence learning with neural networks](#). In *Advances in Neural Information Processing*, pages 3104–3112.
- Stephan Vogel, Hermann Ney, and Christoph Tillmann. 1996. [HMM-based word alignment in statistical translation](#). In *COLING 1996 Volume 2: The 16th International Conference on Computational Linguistics*.
- R. L. Weide. 1998. [The Carnegie Mellon pronouncing dictionary](#).
- Ronald J. Williams. 1992. [Simple statistical gradient-following algorithms for connectionist reinforcement learning](#). In *Reinforcement Learning*, pages 5–32. Springer.
- Kelvin Xu, Jimmy Ba, Ryan Kiros, Kyunghyun Cho, Aaron C. Courville, Ruslan Salakhutdinov, Richard S. Zemel, and Yoshua Bengio. 2015. [Show, attend and tell: Neural image caption generation with visual attention](#). In *Proceedings of the 32nd International Conference on Machine Learning*, pages 2048–2057.
- Kaisheng Yao and Geoffrey Zweig. 2015. [Sequence-to-sequence neural net models for grapheme-to-phoneme conversion](#). In *INTERSPEECH*, pages 3330–3334, Dresden, Germany.
- Min Zhang, Haizhou Li, Rafael E. Banchs, and A Kumar. 2015. [Whitepaper of NEWS 2015 shared task on machine transliteration](#). In *Proceedings of the Fifth Named Entity Workshop*, pages 1–9, Beijing, China. Association for Computational Linguistics.

Small														
	①		④		②		③		④		Ⓜ		Ⓜ	
	WER	PER												
CMUDict	36.2	0.086	31.0	0.074	35.1	0.083	30.8	0.073	30.5	0.072	31.2	0.074	32.0	0.075
NETtalk	31.2	0.075	30.2	0.075	29.6	0.074	29.8	0.074	28.8	0.073	30.3	0.078	35.7	0.088

Large														
	①		④		②		③		④		Ⓜ		Ⓜ	
	WER	PER												
CMUDict	32.3	0.076	31.4	0.073	36.7	0.087	30.5	0.073	29.8	0.071	31.8	0.077	30.5	0.072
NETtalk	29.3	0.071	29.4	0.072	29.5	0.075	26.8	0.068	26.6	0.066	27.7	0.071	29.3	0.072

Table 6: Full breakdown of G2P

A MFS

We consider the following evaluation metrics:

$$\text{LCS}(c_i, r_i) = \frac{1}{2}(|c_i| + |r_i| - \text{ED}(c_i, r_i)) \quad (12a)$$

$$R_i = \frac{\text{LCS}(c_i, r_i)}{|r_i|} \quad (12b)$$

$$P_i = \frac{\text{LCS}(c_i, r_i)}{|c_i|} \quad (12c)$$

$$\text{FS}_i = 2 \frac{R_i \times P_i}{R_i + P_i} \quad (12d)$$

where r_i and c_i is the i^{th} reference and prediction and $\text{ED}(c_i, r_i)$ is the edit distance between c_i and r_i .

B Full breakdown of experiments

A full breakdown of **G** and **T** can be found in Tab. 6 and Tab. 7, respectively. A full breakdown of **I** can be found in Tab. 8 and Tab. 9.

Small														
	①		④		②		③		④		Ⓜ		Ⓜ	
	ACC	MFS												
ArEn	54.9	0.954	54.8	0.953	53.9	0.954	53.5	0.951	56.6	0.954	53.9	0.950	60.1	0.980
EnBa	38.4	0.916	38.9	0.915	38.5	0.914	37.6	0.918	39.7	0.918	38.0	0.909	37.4	0.961
EnHi	42.4	0.922	44.0	0.925	40.8	0.921	46.1	0.927	43.8	0.926	43.6	0.924	43.0	0.967
EnJa	40.5	0.871	40.6	0.868	35.4	0.853	41.2	0.872	41.3	0.872	35.2	0.852	39.4	0.952
EnKa	34.8	0.910	35.5	0.912	33.1	0.909	37.8	0.913	36.0	0.909	34.9	0.907	35.6	0.960
EnKo	52.4	0.861	51.8	0.857	49.1	0.850	54.4	0.861	54.9	0.867	48.9	0.849	47.5	0.958
EnPe	28.3	0.899	32.6	0.908	30.8	0.903	34.8	0.911	30.5	0.901	29.6	0.898	34.7	0.964
EnTa	36.8	0.921	38.7	0.925	36.7	0.918	38.5	0.923	36.2	0.923	37.5	0.921	37.5	0.963
EnTh	42.4	0.909	42.6	0.907	37.0	0.892	42.8	0.907	42.1	0.906	37.1	0.890	40.1	0.954
JnJk	18.1	0.717	18.1	0.717	13.4	0.693	15.3	0.706	18.1	0.716	15.5	0.705	12.7	0.933
ThEn	39.2	0.912	40.2	0.913	31.1	0.882	38.9	0.911	38.6	0.912	33.6	0.897	38.3	0.960
Large														
	①		④		②		③		④		Ⓜ		Ⓜ	
	ACC	MFS												
ArEn	52.2	0.954	54.3	0.954	0.7	0.682	55.4	0.954	55.6	0.953	57.1	0.955	59.7	0.979
EnBa	39.0	0.914	39.2	0.918	40.4	0.917	38.5	0.916	38.2	0.917	37.8	0.912	37.7	0.962
EnHi	42.0	0.923	43.0	0.926	38.9	0.914	45.7	0.929	46.1	0.928	40.7	0.916	45.0	0.968
EnJa	40.8	0.873	40.9	0.872	37.8	0.860	41.6	0.875	40.6	0.872	39.1	0.864	41.1	0.953
EnKa	36.2	0.913	37.9	0.914	35.0	0.909	37.5	0.913	38.6	0.915	38.2	0.913	39.2	0.961
EnKo	53.3	0.868	53.1	0.865	50.7	0.858	53.9	0.866	55.3	0.868	49.7	0.850	50.1	0.961
EnPe	34.0	0.911	34.6	0.913	32.5	0.906	34.2	0.912	35.3	0.911	33.4	0.911	34.3	0.964
EnTa	39.1	0.925	37.6	0.922	32.5	0.901	38.5	0.925	40.2	0.927	37.1	0.919	40.3	0.965
EnTh	43.6	0.910	43.7	0.909	32.5	0.869	43.7	0.909	43.9	0.910	40.0	0.897	41.3	0.955
JnJk	18.1	0.721	18.4	0.721	0.1	0.483	17.2	0.721	17.6	0.720	0.2	0.458	12.6	0.934
ThEn	40.2	0.915	40.3	0.915	37.7	0.909	39.2	0.915	40.3	0.916	32.9	0.897	39.8	0.962

Table 7: Full breakdown of NEWS2015

Small														
	①		②		③		④		Ⓜ		Ⓜ		Ⓜ	
	ACC	MLD	ACC	MLD										
albanian-high	97.2	0.048	98.5	0.023	97.9	0.043	98.1	0.031	98.1	0.045	98.5	0.029	94.5	0.150
arabic-high	89.2	0.396	79.1	0.792	91.0	0.419	90.4	0.360	91.7	0.377	90.2	0.438	89.1	0.340
armenian-high	94.6	0.106	95.3	0.086	90.1	0.214	95.2	0.080	95.5	0.080	93.7	0.126	94.4	0.108
basque-high	100.0	0.000	100.0	0.000	100.0	0.000	99.0	0.010	97.0	0.060	100.0	0.000	95.0	0.140
bengali-high	98.0	0.060	98.0	0.060	99.0	0.030	99.0	0.050	97.0	0.090	98.0	0.080	98.0	0.040
bulgarian-high	88.9	0.165	88.3	0.188	96.1	0.067	94.1	0.101	93.9	0.115	95.4	0.077	96.5	0.058
catalan-high	96.8	0.083	96.9	0.083	96.8	0.075	97.5	0.063	97.2	0.073	97.3	0.068	96.3	0.076
czech-high	90.3	0.170	92.3	0.145	90.6	0.167	91.9	0.157	92.2	0.139	78.2	0.468	91.4	0.152
danish-high	88.9	0.166	88.9	0.174	90.1	0.151	89.1	0.170	90.2	0.148	91.4	0.132	92.6	0.118
dutch-high	93.7	0.112	94.8	0.100	95.2	0.090	95.2	0.090	94.9	0.086	94.2	0.097	94.8	0.093
english-high	96.1	0.077	96.1	0.071	90.4	0.203	96.5	0.074	95.7	0.078	95.3	0.087	96.3	0.062
estonian-high	95.2	0.109	96.0	0.078	96.4	0.070	96.3	0.090	96.8	0.079	96.2	0.091	93.0	0.145
faroesic-high	79.9	0.420	79.2	0.390	78.4	0.449	79.5	0.413	82.9	0.365	81.6	0.392	82.5	0.333
finnish-high	86.6	0.318	81.9	0.278	86.5	0.216	88.2	0.202	90.2	0.271	84.1	0.311	86.1	0.227
french-high	84.5	0.291	85.3	0.270	85.2	0.292	83.8	0.317	85.7	0.262	82.3	0.332	86.5	0.253
georgian-high	97.6	0.039	95.4	0.083	97.8	0.037	97.9	0.113	97.5	0.046	98.2	0.039	97.3	0.038
german-high	89.6	0.244	88.4	0.272	88.1	0.282	89.6	0.257	89.3	0.179	83.7	0.381	88.9	0.276
haida-high	97.0	0.040	98.0	0.030	98.0	0.030	99.0	0.020	97.0	0.040	98.0	0.030	92.0	0.150
hebrew-high	99.0	0.010	98.8	0.013	99.1	0.010	97.5	0.027	97.8	0.027	97.8	0.026	98.7	0.016
hindi-high	95.1	0.482	99.9	0.002	100.0	0.000	100.0	0.000	100.0	0.000	100.0	0.000	99.4	0.014
hungarian-high	83.4	0.338	83.9	0.336	85.2	0.333	82.5	0.372	82.3	0.381	83.2	0.444	83.0	0.367
icelandic-high	82.2	0.333	82.0	0.350	84.1	0.305	84.5	0.304	86.3	0.286	84.4	0.296	84.5	0.300
irish-high	87.4	0.387	84.4	0.454	89.0	0.333	87.9	0.351	90.6	0.289	88.3	0.332	88.5	0.335
italian-high	96.1	0.101	87.2	0.251	96.0	0.099	95.5	0.111	95.7	0.106	95.5	0.105	94.6	0.120
khaling-high	99.2	0.008	98.9	0.018	98.7	0.016	98.0	0.030	98.7	0.018	98.7	0.024	98.1	0.028
kurmanji-high	94.2	0.123	93.7	0.101	92.3	0.184	93.2	0.126	93.8	0.098	93.1	0.143	94.0	0.074
latin-high	65.4	0.578	65.9	0.591	69.6	0.516	70.1	0.476	72.1	0.458	68.6	0.503	70.7	0.450
latvian-high	94.7	0.084	95.3	0.071	93.7	0.104	95.1	0.090	95.5	0.081	94.2	0.101	93.6	0.100
lithuanian-high	87.0	0.178	87.8	0.247	84.9	0.233	86.9	0.196	89.1	0.162	87.4	0.201	80.9	0.258
lower-sorbian-high	94.6	0.111	93.7	0.112	94.8	0.100	93.4	0.138	95.2	0.096	94.8	0.103	94.2	0.108
macedonian-high	94.1	0.088	94.2	0.089	95.3	0.073	90.7	0.164	93.6	0.102	94.7	0.087	94.9	0.094
navajo-high	84.9	0.446	84.6	0.461	81.2	0.468	86.2	0.332	88.5	0.268	85.1	0.356	79.8	0.450
northern-sami-high	93.9	0.112	94.2	0.099	94.8	0.125	93.6	0.145	95.4	0.089	93.2	0.143	91.8	0.154
norwegian-bokmal-high	86.4	0.220	87.6	0.293	88.4	0.193	89.7	0.172	90.0	0.158	88.2	0.198	90.9	0.156
norwegian-nynorsk-high	71.8	0.454	78.1	0.363	76.5	0.392	77.9	0.378	77.4	0.379	81.0	0.324	88.4	0.197
persian-high	99.4	0.013	99.4	0.013	99.4	0.012	99.1	0.016	98.9	0.017	99.2	0.017	96.8	0.064
polish-high	89.8	0.245	86.5	0.306	82.2	0.424	90.7	0.237	89.9	0.258	88.9	0.297	90.8	0.198
portuguese-high	98.0	0.032	96.3	0.060	96.4	0.056	98.5	0.034	98.9	0.024	97.9	0.036	98.0	0.034
quechua-high	99.4	0.013	97.9	0.045	98.7	0.040	98.2	0.053	99.6	0.020	98.2	0.058	96.4	0.087
romanian-high	83.3	0.649	83.6	0.454	75.6	0.711	81.6	0.482	84.8	0.432	83.8	0.473	84.8	0.404
russian-high	89.4	0.263	86.8	0.303	71.2	0.960	90.1	0.271	90.1	0.242	87.7	0.312	89.8	0.233
serbo-croatian-high	89.6	0.209	86.8	0.241	89.0	0.244	87.2	0.256	89.5	0.236	89.9	0.225	91.8	0.159
slovak-high	90.5	0.155	89.8	0.168	87.2	0.212	91.3	0.145	89.6	0.163	90.2	0.158	92.6	0.128
slovene-high	94.7	0.101	94.1	0.110	95.3	0.094	96.3	0.070	96.2	0.080	94.9	0.114	95.9	0.068
sorani-high	89.3	0.131	90.0	0.124	89.2	0.127	87.7	0.148	88.4	0.149	88.9	0.143	84.0	0.222
spanish-high	95.9	0.080	94.3	0.104	96.0	0.083	95.1	0.105	95.5	0.099	94.6	0.118	94.2	0.099
swedish-high	87.1	0.212	87.2	0.214	87.8	0.208	88.9	0.167	88.7	0.185	69.6	0.880	90.2	0.165
turkish-high	97.1	0.069	96.9	0.078	95.6	0.104	96.8	0.073	95.4	0.099	95.5	0.127	93.3	0.146
ukrainian-high	90.4	0.171	91.1	0.157	89.0	0.188	90.3	0.168	91.8	0.141	91.6	0.139	92.9	0.111
urdu-high	99.4	0.009	99.6	0.007	99.2	0.012	99.5	0.009	99.4	0.009	99.7	0.005	98.2	0.027
welsh-high	96.0	0.070	96.0	0.080	98.0	0.040	96.0	0.070	99.0	0.030	98.0	0.040	98.0	0.040

Table 8: Full breakdown of SIGMORPHON2017 with small model

Large														
	①		②		③		④		⑤		⑥		⑦	
	ACC	MLD	ACC	MLD	ACC	MLD	ACC	MLD	ACC	MLD	ACC	MLD	ACC	MLD
albanian-high	97.9	0.037	96.3	0.066	98.5	0.024	98.0	0.030	98.5	0.028	98.8	0.021	96.1	0.123
arabic-high	90.4	0.496	89.8	0.397	88.4	0.456	89.8	0.358	92.3	0.352	91.9	0.437	90.8	0.267
armenian-high	94.3	0.112	95.6	0.166	94.3	0.106	94.9	0.078	95.8	0.075	94.6	0.095	93.6	0.110
basque-high	100.0	0.000	100.0	0.000	99.0	0.030	100.0	0.000	100.0	0.000	100.0	0.000	99.0	0.020
bengali-high	99.0	0.020	99.0	0.050	99.0	0.050	99.0	0.050	99.0	0.050	95.0	0.150	98.0	0.050
bulgarian-high	95.0	0.079	91.9	0.129	93.6	0.095	96.5	0.059	96.8	0.052	96.5	0.061	96.8	0.057
catalan-high	95.8	0.102	96.9	0.074	97.1	0.068	96.9	0.064	97.9	0.056	97.4	0.064	96.3	0.074
czech-high	89.2	0.184	87.4	0.209	87.8	0.241	90.7	0.176	92.7	0.133	89.7	0.188	92.0	0.140
danish-high	88.3	0.167	87.0	0.282	89.3	0.166	88.6	0.159	91.9	0.121	91.7	0.127	92.2	0.121
dutch-high	93.9	0.109	93.3	0.120	94.2	0.107	94.6	0.099	95.7	0.082	95.8	0.075	95.6	0.078
english-high	95.9	0.082	95.7	0.239	93.1	0.151	95.5	0.081	96.3	0.069	96.0	0.078	96.4	0.055
estonian-high	95.5	0.235	96.9	0.069	96.7	0.069	96.3	0.082	97.6	0.064	96.1	0.086	92.7	0.140
faroesic-high	80.8	0.388	80.7	0.468	80.1	0.374	83.0	0.365	84.3	0.327	82.3	0.371	84.5	0.314
finnish-high	89.7	0.323	86.5	0.196	26.2	4.562	88.5	0.212	92.2	0.137	90.4	0.169	88.0	0.197
french-high	82.2	0.329	83.3	0.316	84.0	0.305	82.9	0.335	85.5	0.274	84.7	0.296	85.6	0.273
georgian-high	97.5	0.043	96.8	0.060	96.9	0.056	96.8	0.064	98.2	0.027	98.4	0.022	98.6	0.018
german-high	87.7	0.459	82.4	0.505	76.5	0.751	87.4	0.309	91.3	0.141	88.7	0.233	89.4	0.244
haida-high	98.0	0.030	98.0	0.030	98.0	0.030	97.0	0.040	98.0	0.030	98.0	0.030	95.0	0.100
hebrew-high	98.5	0.019	99.1	0.011	98.5	0.017	98.6	0.015	98.4	0.018	98.7	0.016	98.5	0.018
hindi-high	100.0	0.000	99.7	0.099	99.9	0.001	99.8	0.002	99.9	0.003	100.0	0.000	99.8	0.006
hungarian-high	82.7	0.361	82.0	0.362	81.7	0.400	79.0	0.437	84.1	0.347	82.0	0.386	84.7	0.329
icelandic-high	82.6	0.341	84.4	0.309	82.9	0.338	84.7	0.301	88.0	0.244	87.6	0.248	87.6	0.245
irish-high	85.8	0.377	86.4	0.391	81.8	0.512	88.7	0.423	90.5	0.254	88.3	0.344	89.6	0.304
italian-high	95.8	0.101	96.1	0.089	95.6	0.113	96.6	0.081	96.5	0.084	96.2	0.091	96.0	0.104
khaling-high	99.4	0.006	99.2	0.009	99.4	0.006	99.3	0.009	99.5	0.005	99.4	0.009	97.8	0.031
kurmanji-high	93.0	0.162	93.2	0.268	91.3	0.183	93.1	0.128	93.0	0.089	92.7	0.146	94.0	0.076
latin-high	71.6	0.518	69.6	0.513	70.4	0.485	78.0	0.371	78.4	0.361	76.2	0.392	74.7	0.378
latvian-high	80.8	0.524	91.5	0.133	94.6	0.095	94.3	0.097	96.3	0.056	95.7	0.078	95.2	0.068
lithuanian-high	86.4	0.368	85.4	0.394	87.9	0.173	89.7	0.150	90.6	0.126	90.7	0.139	89.4	0.149
lower-sorbian-high	93.9	0.118	93.7	0.208	95.2	0.094	95.2	0.094	95.1	0.100	96.3	0.073	95.6	0.083
macedonian-high	90.8	0.126	92.7	0.111	94.4	0.085	93.7	0.097	95.9	0.067	94.6	0.085	93.8	0.110
navajo-high	88.1	0.268	86.9	0.312	90.8	0.198	88.3	0.435	91.3	0.201	88.6	0.279	84.5	0.359
northern-sami-high	94.9	0.129	95.8	0.082	95.3	0.121	95.9	0.087	97.5	0.075	96.4	0.103	95.0	0.090
norwegian-bokmal-high	84.4	0.331	85.1	0.403	88.4	0.272	88.1	0.199	88.7	0.190	89.6	0.178	91.0	0.152
norwegian-nynorsk-high	73.3	0.440	76.2	0.408	78.2	0.376	79.4	0.354	80.4	0.345	82.6	0.314	89.3	0.182
persian-high	99.6	0.006	99.2	0.011	99.3	0.108	99.5	0.014	99.3	0.014	99.6	0.011	96.7	0.066
polish-high	85.3	0.406	85.7	0.369	88.5	0.282	88.4	0.366	89.7	0.248	89.2	0.251	90.2	0.193
portuguese-high	97.4	0.041	97.4	0.042	98.2	0.034	97.9	0.037	98.3	0.032	98.9	0.023	98.8	0.028
quechua-high	98.9	0.019	97.9	0.059	97.8	0.048	98.6	0.037	98.9	0.032	98.8	0.037	97.7	0.057
romanian-high	84.9	0.594	83.4	0.568	47.1	2.794	85.1	0.457	86.7	0.400	86.8	0.422	86.4	0.450
russian-high	88.0	0.353	85.8	0.458	86.9	0.324	89.8	0.432	90.5	0.244	90.3	0.244	91.2	0.220
serbo-croatian-high	84.9	0.307	85.0	0.277	88.8	0.323	88.8	0.236	90.9	0.187	82.0	0.426	91.4	0.185
slovak-high	87.7	0.214	89.4	0.270	89.2	0.264	89.6	0.186	92.1	0.126	90.4	0.163	92.6	0.129
slovene-high	94.6	0.096	93.2	0.222	94.6	0.102	95.2	0.078	96.1	0.073	94.9	0.097	96.4	0.063
sorani-high	88.8	0.138	88.4	0.144	88.9	0.133	89.4	0.123	90.3	0.121	90.1	0.120	85.9	0.180
spanish-high	94.3	0.092	95.8	0.163	96.1	0.072	96.1	0.075	96.7	0.056	96.2	0.072	95.4	0.079
swedish-high	85.7	0.237	85.0	0.329	79.4	0.529	85.9	0.235	90.9	0.157	89.6	0.170	92.2	0.132
turkish-high	95.9	0.103	94.9	0.226	94.8	0.118	92.4	0.172	97.0	0.063	94.8	0.121	94.3	0.128
ukrainian-high	90.4	0.170	90.3	0.161	90.8	0.148	92.5	0.126	92.9	0.116	93.1	0.114	91.4	0.144
urdu-high	99.3	0.012	99.4	0.010	99.0	0.015	99.6	0.007	99.3	0.014	99.6	0.006	99.1	0.013
welsh-high	96.0	0.060	98.0	0.050	98.0	0.040	97.0	0.050	97.0	0.070	97.0	0.060	97.0	0.060

Table 9: Full breakdown of SIGMORPHON2017 with large model